



28 **Abstract**

29 The climatic response of mountain permafrost and glaciers located in high-elevation mountain areas has major
30 implications for the stability of mountain slopes and related geomorphological hazards, water storage and
31 supply, and preservation of paleoclimatic archives. Despite a good knowledge of physical processes that
32 govern the climatic response of mountain permafrost and glaciers, there is a lack of observational datasets from
33 summit areas. This represents a crucial gap in knowledge and a serious limit for model-based projections of
34 future behaviour of permafrost and glaciers.

35 A new observational dataset is available for the summit area of Mt. Ortles, which is the highest summit of
36 South Tyrol, Italy. This paper presents a series of air, englacial, soil surface and rock wall temperature collected
37 between 2010 and 2016. Details are provided regarding instrument type and characteristics, field methods,
38 data quality control and assessment. The obtained data series are available through an open data repository.

39 In the observation period the mean annual air temperature at 3830 m a.s.l. was between -7.8 and -8.6°C . The
40 most shallow layers of snow and firn (down to a depth of about 10 m) froze during winter. However melt water
41 percolation restored isothermal conditions during the ablation season and the entire firn layer was found at the
42 melting pressure point. Glacier ice is cold, however only from about 30 m depth. Englacial temperature
43 decreases with depth reaching a minimum of almost -3°C close to the bedrock, at 75 m depth. A small glacier
44 located on a rocky ridge of Mt. Ortles at 3470 m a.s.l., without firn cover, was also found in cold conditions
45 from the surface down to a depth of 9.5 m. The mean annual ground surface temperature was negative for all
46 but one monitored sites, indicating cold ground conditions and the existence of permafrost in nearly all debris-
47 mantled slopes of the summit. Similarly, the mean annual rock wall temperature was negative at most
48 monitored sites, except the lowest one at 3030 m a.s.l. This suggests that the rock faces of the summit are
49 affected by permafrost at all exposures.

50
51
52
53
54
55



56 **1. Introduction**

57 High-elevation mountain areas are complex systems influenced by physical processes occurring in the
58 atmosphere, cryosphere and lithosphere. These processes closely interact and govern the energy and mass
59 balance and climatic response of mountain permafrost and glaciers located at high elevation. Their response
60 to climatic changes has important consequences for i) the stability of mountain slopes and related
61 geomorphological hazards (Huggel et al., 2015; Knight and Harrison, 2023), ii) the thermal regime, water
62 storage and stability of mountain glaciers (Deline et al., 2015), iii) the hydrological balance and water supply
63 from glacierized catchments (Irvine-Fynn and Hubbard, 2017), and iv) the formation and preservation of
64 paleoclimatic archives, such as glacier geochemical records (Gabielli et al., 2010).

65 The ongoing atmospheric warming is leading to a deep transformation of these high-elevation systems, which
66 react sensitively to climatic changes. Indeed, the thermal state of the cryosphere is strongly influenced by
67 variations in air temperature, which regulates its energy and mass balance and dynamic behaviour (Harris et
68 al., 2009; Cicoira et al., 2019; Deline et al., 2015). Projections of future global climate indicate further warming
69 in absence of mitigation policies such as the reduction of greenhouse gas emission (IPCC, 2022). For this
70 reason, the current impacts on high-elevation mountain areas are expected to continue and possibly accelerate.
71 Direct observations of the thermal state and response of high-elevation mountain areas are of great importance.
72 Even though the physical processes that govern the energy and mass balance and climatic response of mountain
73 permafrost and glaciers are known, model-based projections of their future behaviour are subject to large
74 uncertainty. This is because the observational datasets required for model calibration and validation are
75 particularly scarce for these summit areas, where model inputs and results are often poorly constrained and
76 extrapolated, in absence of direct observations (Charbonneau et al., 1981; Machguth et al., 2008; Carturan et
77 al., 2012).

78 Thermal observations in high-elevation mountain areas are also of great value for i) improving knowledge on
79 the air temperature variability (e.g. the so-called elevation-dependent warming, Pepin et al., 2015 and 2022),
80 or the glacier cooling effect (Braithwaite et al., 2002), ii) better understanding the relationship between climatic
81 proxies and meteorological variables (e.g. ice cores, Bohleber et al., 2013), iii) evaluating/improving models
82 (e.g. permafrost distribution models, Boekli et al., 2012), iv) biological and biogeochemical studies (e.g.
83 Rathore et al., 2018), and v) setting baseline conditions for future studies and trend analyses.



84 In this paper we present a novel six-year dataset of air, rock, soil surface and englacial temperature collected
85 between 2010 and 2016 on the summit of Mt. Ortles (46.508° N, 10.541° E, 3905 m a.s.l.), in the eastern Italian
86 Alps. These observations were carried out in the framework of the Ortles Project (ortles.org; Gabrielli et al.,
87 2016). This is an international research project, coordinated by the Byrd Polar and Climate Research Center,
88 The Ohio State University (USA) and the Hydrographic Office of the Autonomous Province of Bolzano, with
89 the aim of extracting ice cores from the Alto dell'Ortles Glacier (Oberer Ortlerferner) to be used for
90 paleoclimatic and paleoenvironmental investigations.

91 Here we provide a full description of the experimental site, data-collection methods and equipment, raw data
92 processing and final datasets.

93

94 **2. Site description**

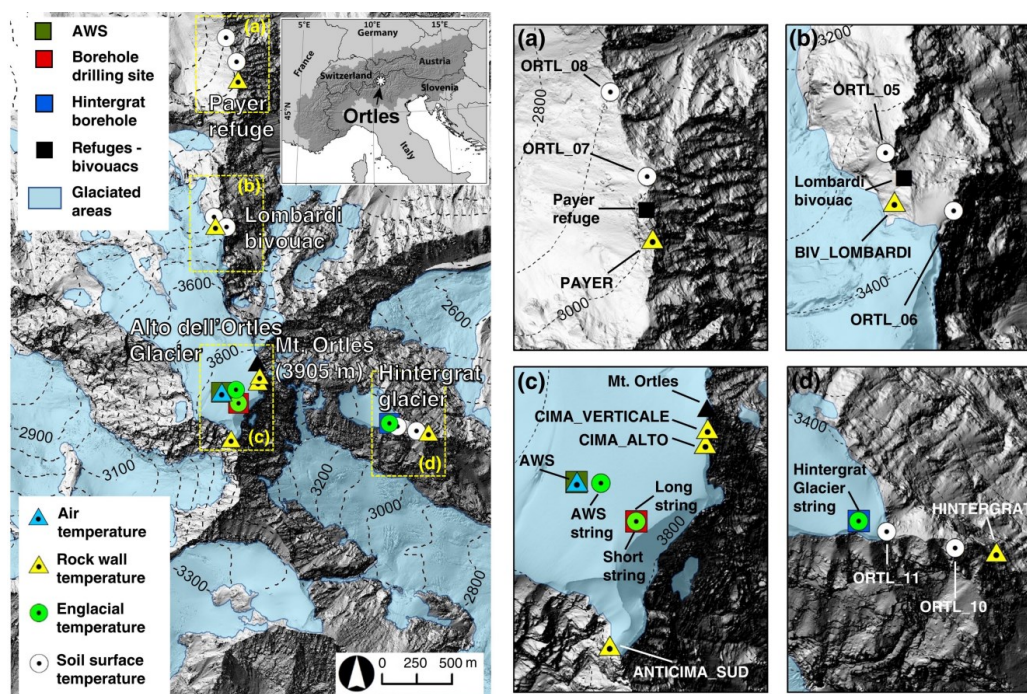
95 Mount Ortles (46.508° N, 10.541° E, 3905 m a.s.l.) is located in the Ortles-Cevedale Mountain Group, which
96 is the largest glacierized area in the Italian Alps (Carturan et al., 2013). It is the highest peak of South Tyrol,
97 in the eastern European Alps (Fig. 1). From a lithological point of view, the summit of Mt. Ortles is mainly
98 composed by dolomites, alternated with dark-stratified limestones and paraconglomeratic limestone levels and
99 breccias. Local outcrops of phyllites rich in quartz and orthogneiss can be found at the base of the mountain
100 (Montrasio et al., 2012).

101 The northern part of the Ortles-Cevedale mountain range is characterised by a continental climate, with scarce
102 annual precipitation (500 mm in the lower valley), which falls mostly in summer. Towards the south, there is
103 an increasing Mediterranean influence and the annual precipitation maxima are in spring and autumn, with
104 cumulative amounts of 900 mm in the lower valleys. In the glaciated areas in the middle of the mountain range,
105 at 3000-3200 m a.s.l., the mean annual precipitation has been estimated between 1400 and 1500 mm (Carturan,
106 2010; Carturan et al., 2012). The mean annual isotherm of 0°C is located at about 2500 m a.s.l. At the elevation
107 of the glaciers (above 3000 m) the snow cover shows a typical annual cycle, with the accumulation season
108 occurring between October and May, and the ablation season between June and September. On the glaciers,
109 however, snowfalls are frequent during summer, especially above 3300-3500 m.

110 Glaciers, glacierets and snowfields cover the Mt. Ortles flanks. Here we describe the two ice bodies
111 investigated in the Ortles Project. The summit area is almost entirely covered by the Alto dell'Ortles Glacier



112 (Oberer Ortlerferner), which is the highest glacier of South Tyrol, ranging in altitude between 3018 and 3905
113 m a.s.l. and covering an area of 1.04 km² (year 2008). The observed glacier thickness is about 75 m (Gabrielli
114 et al., 2012) and the vertical ice profile encompasses the last ~7 kyr (Gabrielli et al., 2016). This glacier is
115 polythermal, with temperate firn and cold ice underneath (Gabrielli et al., 2012). From geomorphological
116 evidence (trimlines and moraines) it is possible to estimate a maximum Little Ice Age (14th - 19th centuries)
117 area of 2.09 km² for this glacier, and a 50% area loss since then. Between 1984 and 2005 the (geodetic) mass
118 balance of the glacier was closer to equilibrium (-0.18 m w.e. y⁻¹) when compared to the majority of glaciers
119 in the Ortles-Cevedale Group in the same period (mean balance rate of -0.69 m w.e. y⁻¹, Carturan et al., 2013).
120 A small glacier, named Hintergrat, covers part of the eastern rocky ridge of Mt. Ortles. The area of this glacier
121 is 0.09 km² and its elevation ranges between 3340 and 3580 m a.s.l. This glacier is mostly in cold thermal
122 conditions and its front hangs over the Fine del Mondo Glacier (Ende der Welt Ferner) underneath.
123 Mountain permafrost is widespread on Mt. Ortles, according to the permafrost distribution modelled by
124 Boeckli et al. (2012), that indicates ‘permafrost in nearly all conditions’ above 2600 m for areas with northern
125 exposure, and above 2900 m for areas with southern exposure.
126 Before the Ortles Project, no specific investigation existed on the air, englacial and permafrost temperatures
127 of this mountain.
128



129

130 Figure 1. Geographic location of Mt. Ortles and of sites instrumented for air, rock, englacial and soil surface
131 temperature measurements. Close ups of the a) Payer Refuge, b) Lombardi Bivouac, c) Mt. Ortles summit
132 area, and d) Hintergrat ridge are reported in the panes on the right. The background hillshaded DEM is from
133 <http://geocatalogo.retecevica.bz.it/>.

134

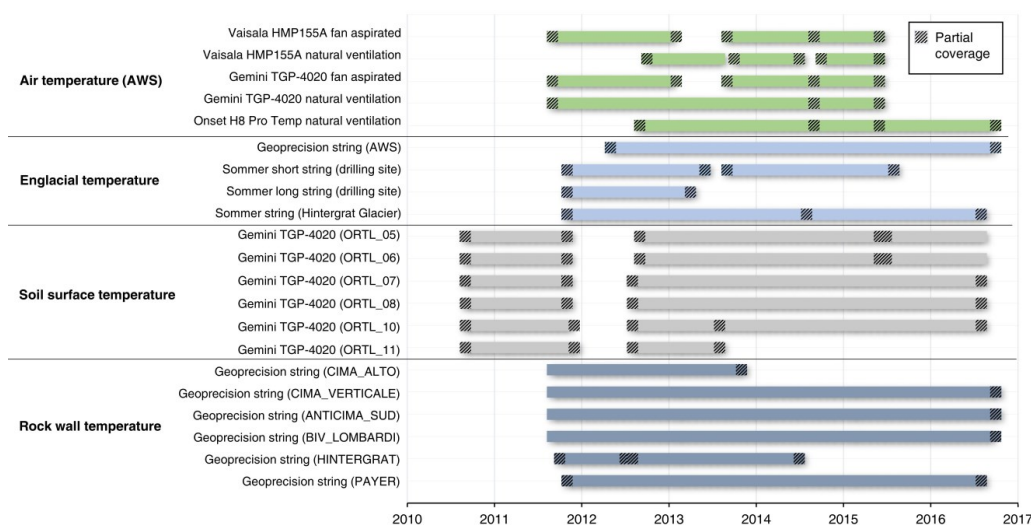
135 3. Data description

136 The temperature datasets presented in this work were obtained by installing stand-alone dataloggers connected
137 to one or several temperature sensors. Due to the remoteness of the study site, dataloggers were powered by
138 lithium or lead-acid batteries, which in the case of the Automatic Weather Station (AWS, Section 3.1) were
139 recharged daily by solar panels. Periodic field visits, mostly performed from June to September, were used for
140 instrumentation maintenance and data download using a laptop. No real-time transmission of data was setup.
141 The dataset is characterised by a good time coverage and a few gaps (Fig. 2), indicating the suitability of the
142 selection of the equipment and field procedures for installation and maintenance. The most significant temporal
143 gaps affect soil surface temperature datasets and were caused by the impossibility of accessing dataloggers in
144 late summer of 2011. Other minor gaps were caused by temporary malfunctions or by damaged equipment,



145 e.g., the rupture of the fan-aspirated radiation shield at the AWS between February and August 2013, which
 146 forced us to treat this period as a data gap. We did not undertake gap-filling, in order to keep the data recorded
 147 in the field as unchanged as possible.
 148 Details of measuring equipment and installations are provided in the following sections. Further details about
 149 the instruments are provided in Table 1 and a topographic description of instrumented sites is reported in Table
 150 E1, in the Appendix. Figures showing examples of data series for each variable are provided in the following
 151 subsections.

152



153

154 Figure 2. Monthly coverage of temperature measurements available from 2010 to 2016 on Mt. Ortles. Partial
 155 coverage indicates the occurrence of data gaps for specific months.

156

157

158 Table 1. Sensor characteristics, setup and period of operation for air, englacial, soil surface and rock wall
 159 temperature measurements on Mt. Ortles.

160

Measured variable	Sensor	Radiation shield	Period of operation		Initial height (m)	Unit	Interval	Integration method and interval	Accuracy
			from	to					
Air temperature data (AWS)									



Air Temperature	Vaisala HMP155A	R. M. Young 43502 fan-aspirated radiation shield	Sep 2011	Jun 2015	+4	°C	15 min	avg 1 h	$\pm(0.226 - 0.0028 \cdot T)$ °C from -80 to 20°C, $\pm(0.055 + 0.0057 \cdot T)$ °C from 20 to 60 °C
Air Temperature	Vaisala HMP155A	Campbell Scientific MET 21 radiation shield with natural ventilation	Sep 2012	Jun 2015	+4	°C	15 min	avg 1 h	$\pm(0.226 - 0.0028 \cdot T)$ °C from -80 to 20°C, $\pm(0.055 + 0.0057 \cdot T)$ °C from 20 to 60 °C
Air Temperature (Backup and comparison)	Gemini TGP-4020	R. M. Young 43502 fan-aspirated radiation shield	Sep 2011	Jun 2015	+4	°C	1 h	avg 1 h	$\pm(0.2 - 0.005 \cdot T)$ °C from -40 to 0°C, ± 0.2 °C from 0°C to 40°C
Air Temperature (Backup and comparison)	Gemini TGP-4020	R.M. Young 41303-5 radiation shield with natural ventilation	Sep 2011	Jun 2015	+4	°C	1 h	avg 1 h	$\pm(0.2 - 0.005 \cdot T)$ °C from -40 to 0°C, ± 0.2 °C from 0°C to 40°C
Air Temperature (Backup and comparison)	Onset Hobo H8 Pro Temp	Davis 7714 radiation shield with natural ventilation	Sep 2012	Sep 2016	+4	°C	1 h	avg 1 h	$\pm(0.63 - 0.022 \cdot T)$ °C from -40 to 0°C, ± 0.63 °C from 0°C to 40°C

Englacial temperature data

Snow and firn temperature at the AWS site	Geoprecision thermistor string (15 sensors)		Jun 2012	Sep 2016	-0.6 / -1.6 / -2.6 / -3.6 / -4.6 / -5.6 / -6.6 / -7.6 / -8.6 / -9.6 / -10.6 / -11.6 / -12.6 / -13.6 / -14.6	°C	2 h	instant 2 h	± 0.5 °C from -10°C to +85°C
Englacial temperature at the borehole drilling site (short string)	Sommer thermistor string (11 sensors)		Nov 2011	Aug 2015	0 / -1 / -2 / -3 / -4 / -6 / -8 / -10 / -15 / -20 / -25	°C	1 h	instant 1h	± 0.1 °C from 0°C to 70°C
Englacial temperature at the borehole drilling site (long string)	Sommer thermistor string (4 sensors)		Nov 2011	Apr 2013	-15 / -35 / -55 / -75	°C	1 h	instant 1h	± 0.1 °C from 0°C to 70°C
Englacial temperature at the Hintergrat Glacier	Sommer thermistor string (5 sensors)		Nov 2011	Aug 2016	-1.5 / -3.5 / -5.5 / -7.5 / -9.5	°C	1 h	instant 1h	± 0.1 °C from 0°C to 70°C

Soil surface temperature data

Soil surface temperature at Lombardi bivouac - ORTL_05	Gemini TGP-4020		Sep 2010	Sep 2016	-0.15	°C	1 h	avg 1h	$\pm(0.2 - 0.005 \cdot T)$ °C from -40 to 0°C, ± 0.2 °C from 0°C to 40°C
Soil surface temperature at Lombardi bivouac - ORTL_06	Gemini TGP-4020		Sep 2010	Sep 2016	-0.12	°C	1 h	avg 1h	$\pm(0.2 - 0.005 \cdot T)$ °C from -40 to 0°C, ± 0.2 °C from 0°C to 40°C
Soil surface temperature at Payer refuge - ORTL_07	Gemini TGP-4020		Sep 2010	Aug 2016	-0.05	°C	1 h	avg 1h	$\pm(0.2 - 0.005 \cdot T)$ °C from -40 to 0°C, ± 0.2 °C from 0°C to 40°C
Soil surface temperature at Payer refuge - ORTL_08	Gemini TGP-4020		Sep 2010	Aug 2016	-0.05	°C	1 h	avg 1h	$\pm(0.2 - 0.005 \cdot T)$ °C from -40 to 0°C, ± 0.2 °C from 0°C to 40°C
Soil surface temperature at Hintergrat ridge - ORTL_10	Gemini TGP-4020		Sep 2010	Aug 2016	-0.05	°C	1 h	avg 1h	$\pm(0.2 - 0.005 \cdot T)$ °C from -40 to 0°C, ± 0.2 °C from 0°C to 40°C
Soil surface temperature at Hintergrat ridge - ORTL_11	Gemini TGP-4020		Sep 2010	Aug 2013	-0.05	°C	1 h	avg 1h	$\pm(0.2 - 0.005 \cdot T)$ °C from -40 to 0°C, ± 0.2 °C from 0°C to 40°C



Rock wall temperature data									
Rock wall temperature at Mt. Ortles summit - CIMA_ALTO	Geoprecision thermistor string (3 sensors)	Sep 2011	Nov 2013	-0.10 / -0.30 / -0.55	°C	1 h	instant 1h	±0.5 °C from -30 to -5 °C, ±0.1 °C from -5 to +40 °C	
Rock wall temperature Mt. Ortles summit - CIMA_VERTICALE	Geoprecision thermistor string (3 sensors)	Sep 2011	Sep 2016	-0.10 / -0.30 / -0.55	°C	1 h	instant 1h	±0.5 °C from -30 to -5 °C, ±0.1 °C from -5 to +40 °C	
Rock wall temperature at Vorgipfel - ANTICIMA_SUD	Geoprecision thermistor string (3 sensors)	Sep 2011	Sep 2016	-0.10 / -0.30 / -0.55	°C	1 h	instant 1h	±0.5 °C from -30 to -5 °C, ±0.1 °C from -5 to +40 °C	
Rock wall temperature at Lombardi bivouac - BIV_LOMBARDI	Geoprecision thermistor string (3 sensors)	Sep 2011	Sep 2016	-0.10 / -0.30 / -0.55	°C	1 h	instant 1h	±0.5 °C from -30 to -5 °C, ±0.1 °C from -5 to +40 °C	
Rock wall temperature at Hintergrat - HINTERGRAT	Geoprecision thermistor string (3 sensors)	Oct 2011	Aug 2014	-0.10 / -0.30 / -0.55	°C	1 h	instant 1h	±0.5 °C from -30 to -5 °C, ±0.1 °C from -5 to +40 °C	
Rock wall temperature at Payer refuge - PAYER	Geoprecision thermistor string (3 sensors)	Nov 2011	Aug 2016	-0.10 / -0.30 / -0.55	°C	1 h	instant 1h	±0.5 °C from -30 to -5 °C, ±0.1 °C from -5 to +40 °C	

161

162

163

164 **3.1 Air temperature data**

165 On 30 September 2011 an Automatic Weather Station (AWS) was installed on the upper accumulation area of
 166 Alto dell'Ortles Glacier, at an elevation of 3830 m a.s.l. The AWS was equipped with a Campbell Scientific
 167 CR-1000 datalogger, solar panels and sensors for air temperature and relative humidity (Vaisala HMP155A),
 168 wind speed and direction (R. M. Young 05103), incoming and outgoing shortwave and longwave radiation
 169 (Delta Ohm LP Pyra 05 and LP PIRG 01), and snow depth (Campbell Scientific SR50A). The equipment was
 170 supported by an aluminum tower (composed of 2-m modules), anchored in the firm at 2 m depth and supported
 171 by wooden boards. After the installation, the tower extended 4 m from the surface. The sensors and solar panels
 172 were fixed on top of the tower, whereas the datalogger/battery housing box was fixed at the bottom (Figs. F1
 173 and F2).

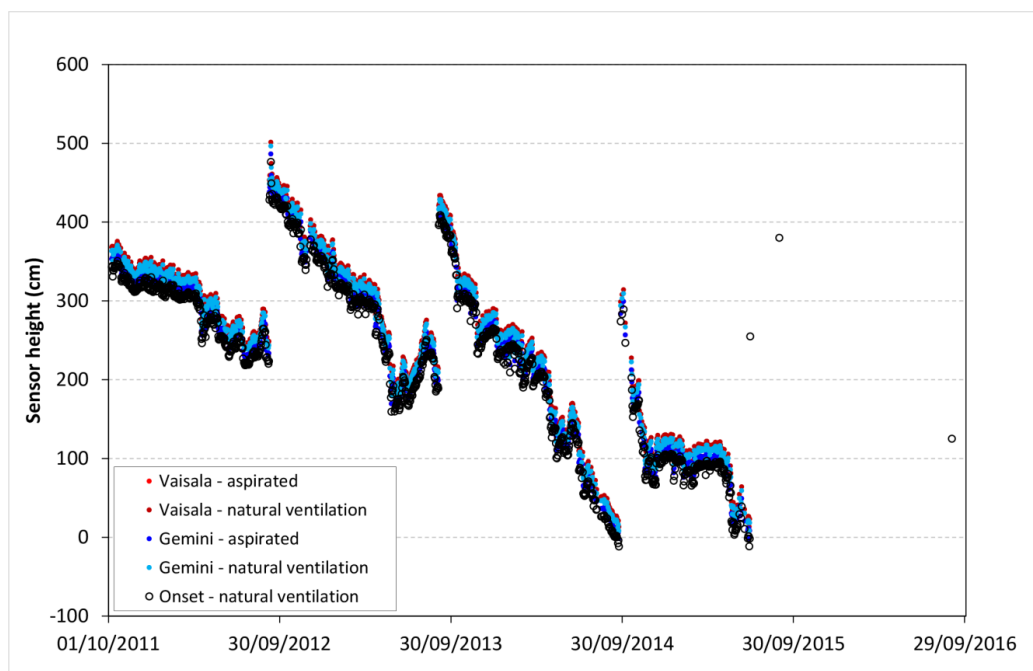
174 The Vaisala HMP155A sensor was installed inside a R. M. Young 43502 fan-aspirated radiation shield. Two
 175 standalone Gemini TGP-4020 dataloggers equipped with PB-5003-1 thermistor probes were also installed for
 176 comparison and backup purposes, one in the same fan-aspirated radiation shield of the Vaisala HMP155A
 177 sensor and one inside a 6-plate R.M. Young 41303-5 radiation shield with natural ventilation. In September



178 2012, we installed an additional HMP155A temperature sensor inside a 15-plate Campbell Scientific MET 21
179 radiation shield with natural ventilation, and an Onset Hobo H8 Pro Temp datalogger housed in an 8-plate
180 Davis 7714 radiation shield with natural ventilation (Figs. F3 and F4). Sensor specifications are reported in
181 Table 1. The Vaisala HMP155A data were recorded as 15-minute mean values, whereas the Gemini TGP-4020
182 dataloggers recorded hourly minimum and maximum temperature, and the Hobo H8 Pro Temp datalogger
183 recorded hourly instantaneous temperature. All the temperature records have been converted into hourly
184 averages, averaging 15-minute means for the Vaisala HMP155A sensors, minimum and maximum hourly
185 temperature for the Gemini TGP-4020 dataloggers, and instantaneous temperature at the beginning and at the
186 end of each hour for the Hobo H8 Pro Temp datalogger, assuming a linear variation of temperature during
187 each hour.

188 All the air temperature sensors were installed at the same level (± 20 cm). The height of the air temperature
189 sensors above the glacier surface changed with the snow accumulation over time. To prevent burial by snow
190 accumulation, the tower was elongated annually by adding a 2-m module. Figure 3 shows the height of the
191 sensors above the glacier surface, as reconstructed from the snow depth data and maintenance logs (Table D1).

192



193



194 Figure 3. Air temperature sensors height above the snow surface.

195

196

197 Despite the remote and harsh environment, the AWS worked properly without major interruptions. In June

198 2015 it was removed, but the Hobo H8 Pro Temp logger was left on site and recorded additional 15 months of

199 data. The main issue linked to the specific environment of installation was ice and snow accretion combined

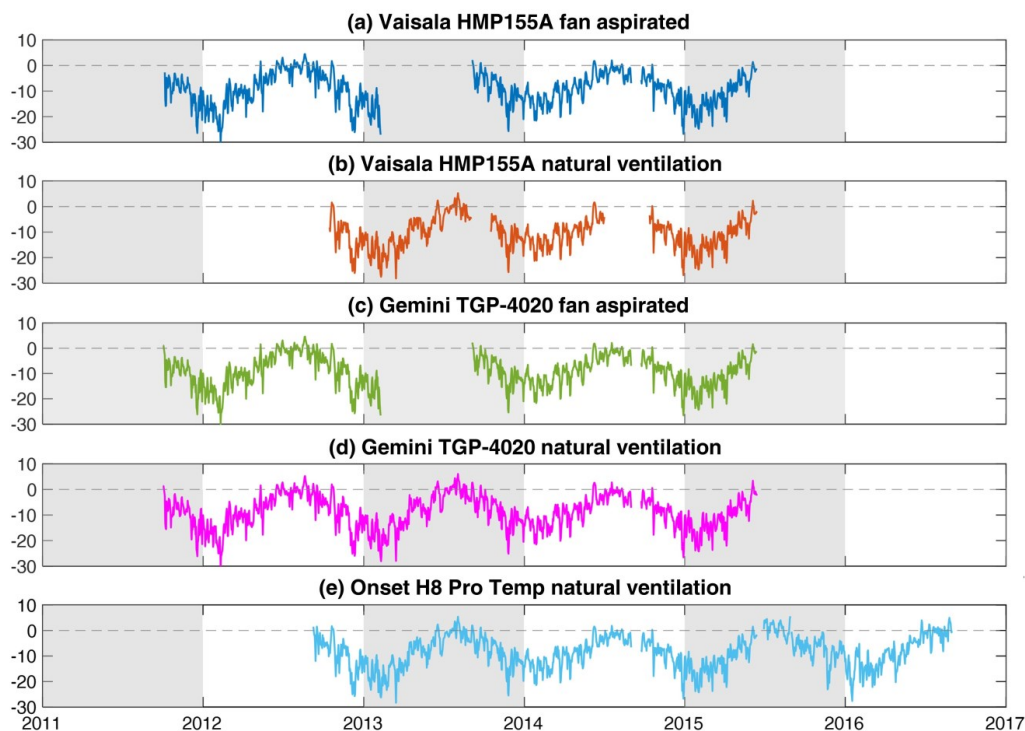
200 with strong winds, which damaged the fan-aspirated radiations shield in February 2013. The obtained data are

201 shown in Fig. 4.

202

203

Air temperature (AWS) [°C]



204

205 Figure 4. Daily mean air temperature series measured by different sensors installed at the Automatic Weather

206 Station on Mt. Ortles.

207



208 **3.2 Englacial temperature data**

209 Englacial temperature measurements were collected at three different sites on Mt. Ortles: i) at the AWS site
210 (3830 m), ii) at the borehole drilling site (3859 m), and iii) at the Hintergrat glacier (3476 m). The obtained
211 englacial temperature data are shown in Fig. 5.

212

213 **3.2.1 Snow and firn temperature data at the AWS site**

214 On the 18th of June 2012 a 20-meter thermistor string manufactured by Geoprecision GmbH (Germany) was
215 installed 10 m east of the AWS (Fig. F1). The thermistor string was composed of a Dallas M-Log5W
216 datalogger, powered by a 3.6 V lithium battery, and connected to 15 digital Dallas temperature sensors spaced
217 one meter from each other. The string was lowered into a 14.6 m hole drilled using a steam ice drill. The initial
218 depth of temperature sensors ranged between 0.6 and 14.6 m, and increased afterwards up to about 6 m due to
219 the accumulation of snow. The logger was housed inside a plastic box on the glacier surface, subsequently
220 buried in the snow. Instantaneous temperature data were recorded with a 2-hour frequency.

221 The data were retrieved by means of a laptop using a USB dongle connected wireless (radio transmission) to
222 the logger, below the glacier surface. We were able to retrieve temperature data with the logger buried below
223 a maximum of ~6 m of snow and firn. The thermistor string worked properly without interruptions and without
224 requiring maintenance or battery replacement. Sensor specifications are reported in Table 1.

225

226 **3.2.2 Englacial temperature at the borehole drilling site**

227 The site where the Ortles Project deep ice cores were extracted is a small col (3859 m; 10°32'34", 46°30'25")
228 between the summit of Mt. Ortles and the Anticima Sud/Vorgipfel (3845 m, Figs. 1 and G1). The ice is 75 m
229 thick at this site as indicated by geophysical sensing prospecting and confirmed by ice core drilling operations
230 (Gabielli et al., 2016). Two thermistor strings were installed in borehole number 3 on the 5th of October 2011,
231 immediately after the completion of the drilling operations (Fig. G3a). The strings were composed of an MDL
232 8/3 datalogger, manufactured by Sommer GmbH & Co KG (Austria). The logger was connected to 44031
233 thermistors, manufactured by ThermX (USA).



234 A first (short) thermistor string was 35 m long, and was equipped with temperature sensors at 0, 1, 2, 3, 4, 6,
235 8, 10, 15, 20, 25 m (initial depth). The other (long) string was 100 m, with temperature sensors at 15, 35, 55
236 and 75 m (initial depth). Burial depth of sensor increased over time due to net snow and firn accumulation.
237 Dataloggers and exceeding portions of strings were housed inside a metal box and arranged on a winding
238 system (Fig. G3), making it possible to extend the thermistor strings and to arise the box at the glacier surface
239 periodically. Field maintenance was also required to replace batteries and download the stored data.
240 Instantaneous temperature data were recorded with a 1-hour frequency.
241 The short string worked properly until removal in summer 2015, with the exception of a two-month gap in
242 summer 2013. The long string stopped working in April 2013, possibly due to ice dynamics and deformation
243 of the borehole at a depth below 25-30 m. Sensor specifications are reported in Table 1.

244

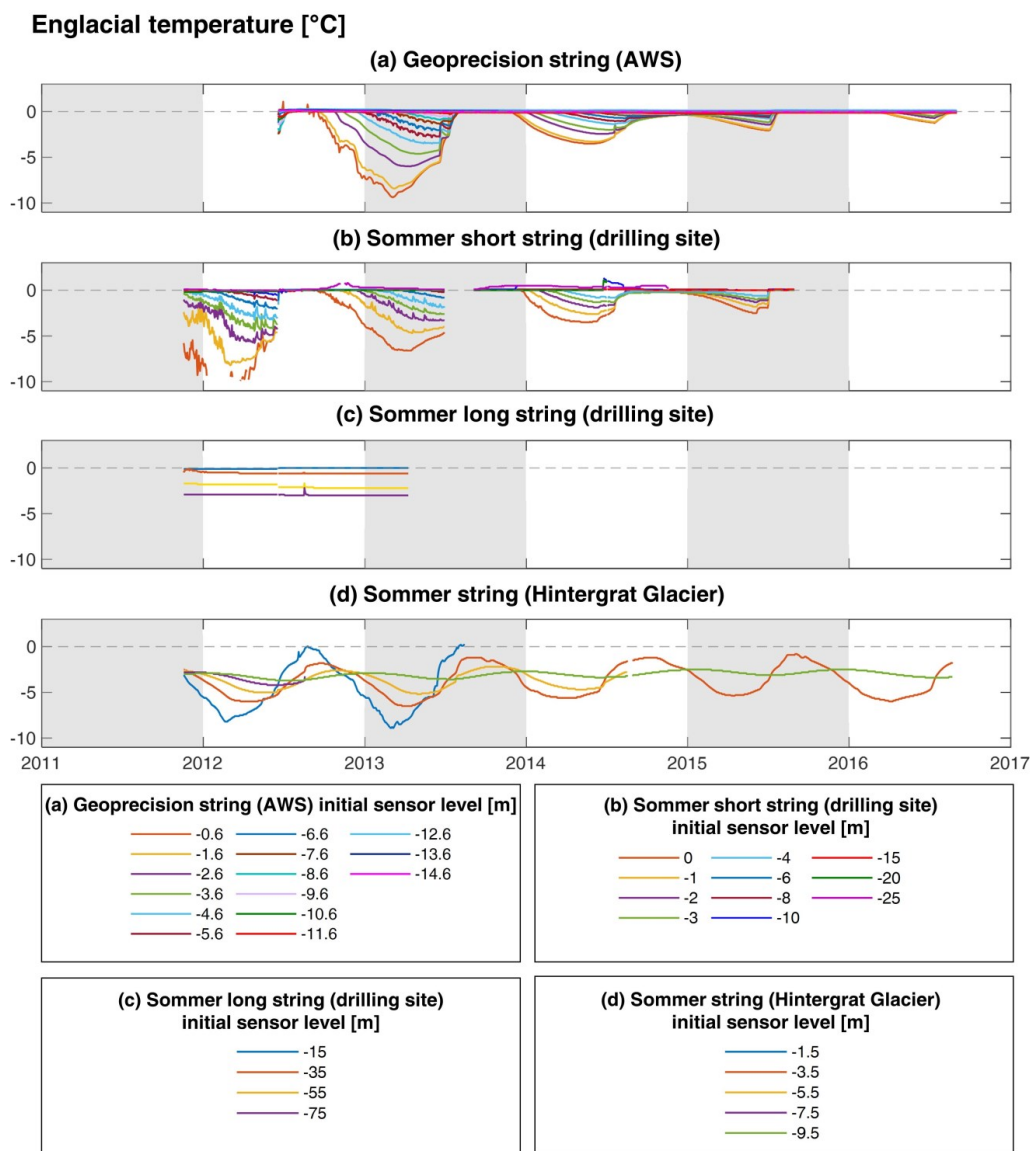
245 3.2.3 Englacial temperature at the Hintergrat Glacier

246 On the 14th of October 2011 a thermistor string was installed at 3476 m a.s.l. on top of the Hintergrat Glacier
247 (Fig. G2). The string was manufactured by Sommer GmbH & Co KG (Austria), with the same components as
248 those installed at the ice core drilling site (Section 3.2.2, Fig. G4). It was lowered into a hole drilled using a
249 steam ice drill down to a depth of 9.6 m. We did not reach the glacier bottom at this site. The temperature
250 sensors were placed at 1.5, 3.5, 5.5, 7.5 and 9.5 m below the glacier surface. This lower site is subject to net
251 ablation, therefore in this case the initial depth decreased through time and the sensor at 1.5 m depth came to
252 the surface in summer 2013. After 2013, this sensor's data were consequently discarded.

253

254

255



256

257 Figure 5. Englacial temperature measured at various sites and various depths on the Alto dell'Ortles Glacier.

258

259

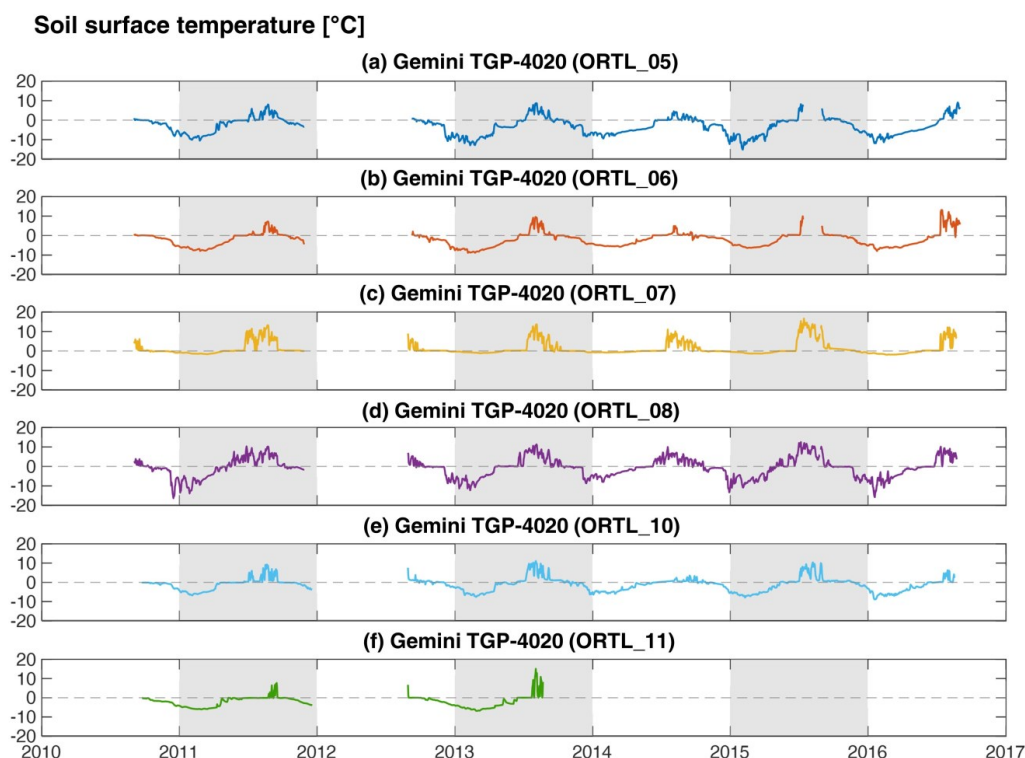
260 3.3 Soil surface temperature data

261 The thermal regime of the soil surface at six deglaciated sites on Mt. Ortles was monitored using standalone

262 temperature dataloggers over the period between September 2010 and September 2016. We used Gemini TGP-



263 4020 dataloggers, powered by 3.6 V lithium batteries, and equipped with PB-5001 probes, which were placed
264 5-15 cm below the soil surface (Figs. H1 and H2). Mean temperature data were recorded at hourly intervals.
265 Periodic maintenance was required to download the data and replace exhausted batteries.
266 The monitored sites range in elevation between 2899 and 3466 m a.s.l. The dataloggers were placed in pairs
267 at three main locations (Figs. 1 and H3): refuge Payer (ORTL_07 and ORTL_08), bivouac Lombardi
268 (ORTL_05 and ORTL_06) and Hintergrat ridge (ORTL_10 and ORTL_11).
269 The data series extend from late summer 2010 to late summer 2016, with a gap between autumn 2011 and late
270 summer 2012 and for ORTL_05 and ORTL_06 also between July and August 2015, due to the impossibility
271 of accessing the dataloggers for maintenance. ORTL_11 was buried under snow and firn after 2013 and has
272 never been recovered. The obtained soil surface temperature data are displayed in Fig. 6.
273



274

275 Figure 6. Soil surface temperature data measured at various locations on Mt. Ortles.

276



277

278

279 **3.4 Rock wall temperature data**

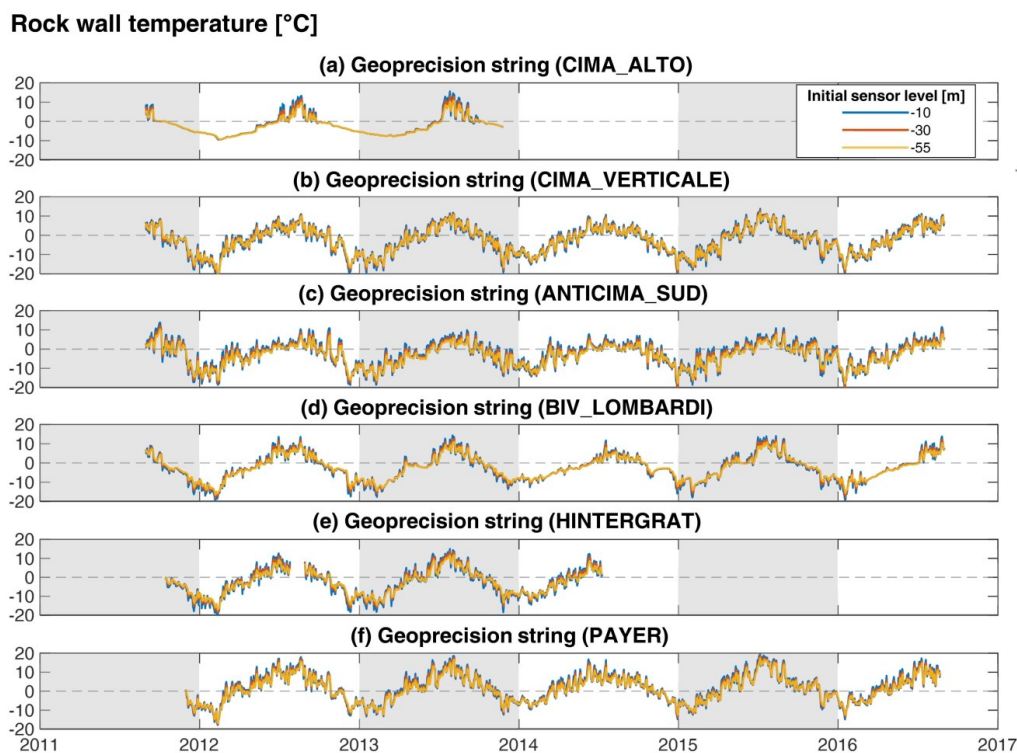
280 The sub-surface temperature of rock walls located at six sites on Mt. Ortles was monitored starting in late
281 summer and autumn 2011 (Fig. 2). Very steep/almost vertical rock walls with different exposures and
282 elevations were selected for monitoring (Figs. 1 and I3). Two sites were established next to the Mt. Ortles
283 summit (3900 and 3880 m, facing East), one at the Vorgipfel (3844 m, facing South), one at the Hintergrat
284 (3370 m, facing North-East), one at the bivouac Lombardi (3351, facing West) and one at the refuge Payer
285 (3030 m, facing East).

286 Rock temperature data were acquired using Geoprecision Dallas M-Log5W dataloggers, powered by a 3.6 V
287 lithium battery, and connected to three digital Dallas temperature sensors installed at 0.1, 0.3 and 0.55 m depth,
288 into holes drilled with a hammer drill (Fig. I1). Instantaneous temperature data were stored at hourly intervals
289 and downloaded with a remote connection using a wireless USB dongle and a laptop (Fig. I2).

290 The datalogger placed at the Hintergrat was damaged by hikers in late July 2012. After the damage was
291 repaired in late August 2012 it was operational until August 2014 when it was again found badly damaged and
292 therefore it was removed.

293 One of the loggers installed at the Mt. Ortles summit ("CIMA_ALTO") stopped working in November 2013
294 due to battery failure, the other dataloggers worked properly until the end of the monitoring period, in late
295 summer 2016. Sensor specifications are reported in Table 1. The obtained rock wall temperature data are
296 displayed in Fig. 7.

297



299 Figure 7. Rock wall temperature measurements at various sites and three depths on Mt. Ortles.

300

301 4. Data quality control and assessment

302 The temperature datasets presented in this work were carefully inspected to detect possible problems affecting
303 raw measurements and to ensure the highest possible accuracy. Data quality controls allowed assigning a
304 quality flag to each temperature record, as described in Table B1.

305 Air temperature sensors were exposed to harsh conditions, without protection from snow, rock or firn/ice as in
306 the case of sensors used to measure the englacial, soil and rock wall temperature. For this reason, the air
307 temperature sensors were subjected to possible damage by strong winds and lightning, ice and snow accretion,
308 and burial by snow in case of abundant snowfall. In addition, they were subjected to the typical issues affecting
309 air temperature measurements, arising from low wind speed and high solar radiation, worsened by high surface
310 albedo, which generally lead to errors due to heating during daytime (WMO, 2021). Sensor drifting should
311 also be taken into account as a potential problem.



312 In order to spot problematic periods we carried out a sensor-by-sensor intercomparison, calculating hourly and
313 daily temperature differences among pairs of sensors, including data from two neighbouring weather stations
314 (Madriccio, 2825 m a.s.l., and Cima Beltovo, 3328 m a.s.l., Weather Service - Autonomous Province of
315 Bozen/Bolzano) for additional confirmation. We compared temperature difference series with maintenance
316 logs, to understand the sources of malfunctions and anomalies, and to assign data quality flags to air
317 temperature series. Data recorded during malfunctions were handled as data gaps and removed from the
318 published series. Anomalies in periods of heavy snowfalls, which caused snow/ice accretion and a rapid
319 decrease of sensor height, are flagged with a specific code (Table B1).

320 Englacial and rock wall temperature were checked in the same way by calculating hourly and daily differences
321 among sensors located at the same site, and checking irregularities (i.e. sudden jumps in temperature
322 differences) in combination with field observations during maintenances. We have detected no malfunctions,
323 but it is possible that after maintenance operations (detailed in Table D1 to D4) a short period of a few hours
324 or a few days was required to reach a new equilibrium at englacial temperature monitoring sites. We have
325 highlighted these maintenance operations with potential impacts on measured temperature using a data quality
326 code, reported in Table B1.

327 Soil surface temperature data displayed no obvious anomalies and were checked in the ‘zero-curtain’ phase,
328 that is the 0°C plateau during the snowmelt phase. Only ORTL_07 required a correction of measured
329 temperature in 2014 (offset applied = -0.35°C) and 2015 (offset applied = -1.1°C), to correct discrepancies
330 larger than sensor accuracies reported in Table 1. We have highlighted these adjustments with a quality flag in
331 the corresponding data files (Table B1).

332

333 **5. Data availability**

334 The datasets from this study are publicly available at <https://doi.org/10.5281/zenodo.7879969> (Carturan et al.,
335 2023). The data files are stored in Microsoft Excel .xlsx format. Detailed information on the file content and
336 structure is reported in the Appendix of this manuscript (Tables A1, B1 and C1).

337

338

339



340 **6. Summary of observations and research outlook**

341 The datasets collected on Mt. Ortles enable description of its thermal state within a time window of six years
 342 (2011-2016). This period is long enough to provide a picture of modern average conditions and interannual
 343 variability, and as such, it is useful as a baseline for possible future studies aimed at detecting changes and
 344 trends in monitored variables.

345 In the period from 02-10-2011 to 01-09-2016, the mean daily air temperature ranged between -30.1°C (12-02-
 346 2012) and 6.1°C (03-08-2013), averaging -8.3°C. These statistics have been extracted from a merged time
 347 series, which combines the sensors that have the longest time coverage (Fig. 2), i.e. the GEMINI TGP-4020
 348 with natural ventilation before 15-06-2015 and the ONSET Hobo H8 (natural ventilation) from 15-06-2015.
 349 The air temperature reached hourly extremes of -33.3°C (09-02-2012 at 24:00 UTC) and 10.1°C (20-08-2012
 350 at 10:00 UTC). These extremes must be viewed with caution due to the high sensitivity of short-term
 351 temperature fluctuations to possible errors, mainly due to low natural ventilation. The aspirated shield installed
 352 at the weather station proved subject to damage and malfunction. However, it was operational at the time when
 353 the two extreme values were recorded, providing identical minimum temperature of -33.3°C, and a maximum
 354 of 8.0°C at 13:00 of 20-08-2012. In the common period of operation, the average difference in mean daily air
 355 temperature among pairs of installed sensors did not exceed 0.60°C in absolute value (Table 2).

356

357 Table 2. Average difference in mean daily air temperature among pairs of installed sensors for air temperature
 358 measurements (f.a. = fan-aspirated; n.v. = natural ventilation). Differences are calculated in the common
 359 working period for pairs of sensors, i.e. they refer to different periods (overlaps are shown in Fig. 4). Column
 360 headings represent the first term of the difference calculation.

361

	Vaisala HMP155A (f.a.)	Vaisala HMP155A (n.v.)	Gemini TGP- 4020 (f.a.)	Gemini TGP- 4020 (n.v.)	Onset Hobo H8 Pro Temp (n.v.)
Vaisala (f.a.) HMP155A		-0.28	0.11	0.18	-0.02
Vaisala (n.v.) HMP155A			0.41	0.60	0.32
Gemini (f.a.) TGP-4020				0.08	-0.15



Gemini TGP-4020
 (n.v.) -0.28

362

363

364 The mean daily air temperature was above 0°C for 39 days in 2012, 48 in 2013, 15 in 2014, 44 in 2015, and
 365 31 in 2016. These results highlight a significant interannual variability in the length of the melt season at this
 366 high-elevation site. The mean annual air temperature averaged -8.3°C, ranging between -8.6°C in 2012 and
 367 2013, and -7.8°C in 2016 (Table 3).

368

369 Table 3. Mean annual air temperature recorded at the automatic weather station on Mt. Ortles, with five
 370 different sensors (f.a. = fan-aspirated; n.v. = natural ventilation). The mean temperature is reported only for
 371 years with less than one month missing of data, and is calculated between the 1st of September and the 31st of
 372 August.

373

Sensor	Vaisala HMP155A (f.a.)	Vaisala HMP155A (n.v.)	Gemini TGP- 4020 (f.a.)	Gemini TGP- 4020 (n.v.)	Onset Hobo H8 Pro Temp (n.v.)	Merged (n.v.)
Year						
2012	-8.9		-8.7	-8.6		-8.6
2013				-8.6	-9.0	-8.6
2014	-8.4		-8.2	-8.1	-8.4	-8.1
2015					-8.6	-8.3
2016					-8.1	-7.8

374

375 Englacial temperature measurements reveal warm firm and isothermal summer conditions down to a depth of
 376 25 m on the upper part of the Alto dell'Ortles Glacier. The summer was cold (and snowy) enough only in 2014
 377 to preserve below-zero temperature in firm and snow down to a depth of about 15 m at the AWS and 10 m at
 378 the drilling site. On the other hand deep borehole data available until 10/04/2013 confirm that glacier ice below
 379 the firm-ice transition is cold throughout the year, as detected during ice coring operations at the drilling site in
 380 October 2011 (Gabrielli et al. 2012). The ice temperature decreases with depth reaching a minimum of -3°C
 381 at the glacier bed, at 75 m below the surface, and does not change significantly throughout the year.



382 The Hintergrat glacier is also composed of cold ice, which is subject to net surface ablation at the string
383 installation site. Indeed, the sensor at 1.5 m initial depth was exposed at the surface in August 2013. A 1.2 m
384 layer of firm formed in 2014, but underwent complete ablation by the end of the following summer.
385 Soil surface temperature measurements, and in particular the mean annual ground surface temperature
386 (MAGST, Table 4), suggest the existence of permafrost on most of the monitored sites (Guglielmin et al.,
387 2003; Ballantyne, 2018), with the exception of the ORTL07 site which is at 2994 m a.s.l, close to the Payer
388 refuge (Fig. 1). The results of ORTL_10 and ORTL_11 can be compared to analogous observations
389 (unpublished) carried out in the same period on Mt Vioz (3520 m a.s.l., 14 km south of Mt. Ortles), using the
390 same devices and field techniques at two sites with similar elevation and exposure. On Mt. Vioz the MAGST
391 was -2.1°C for the site with southern exposure and -2.9°C for the site with eastern exposure, indicating slightly
392 colder soil surface thermal conditions.

393

394 Table 4. Mean annual ground surface temperature (MAGST) recorded at six different sites on Mt. Ortles. Site
395 locations are reported in Fig. 1. MAGST is reported only for years with less than one month of missing data,
396 and is calculated between the 1st of September and the 31st of August.

397

Sensor	ORTL_05	ORTL_06	ORTL_07	ORTL_08	ORTL_10	ORTL_11
Year						
2011	-2.6	-2.4	1.3	-1.2	-1.2	-2.4
2012						
2013	-3.5	-2.7	1.1	-1.0	-0.7	-2.1
2014	-3.2	-2.1	0.9	-0.5	-1.5	
2015			1.9	-0.3	-1.0	
2016	-3.4	-1.6	0.7	-1.6	-1.9	

398

399

400

401 Rock wall temperature provided results that are in line with soil surface temperature measurements. The
402 warmest site was close to the Payer refuge, with mean annual rock surface temperature (MARST) above the
403 freezing level (Table 5). All the other monitored rock walls displayed below-freezing MARST and similar
404 behaviour, with the exception of CIMA_ALTO, close to the Mt. Ortles summit, where rock temperature
405 fluctuations appear to be dampened by snow accumulation between September and May (Fig. 7).



406 The collected data are being analysed for the interpretation of the ice core drilled in the framework of the Ortles
 407 Project. In particular, air and englacial temperature data are used for developing and validating a model that
 408 aims at reproducing the formation of the isotopic record in snow and firn.
 409 Together with rock wall and soil surface temperature, these datasets represent unique observations at such
 410 elevation in the eastern European Alps, and may contribute to the study and understanding of specific aspects
 411 of the climatic sensitivity of the alpine cryosphere. For example, they can be used for the development of
 412 permafrost distribution and degradation models, air temperature simulations over glacierized areas (including
 413 the so-called glacier cooling effect), snow and glacier mass balance models, glacio-hydrological forecasting
 414 systems, or dynamic glacier models that take into account the thermal state of glaciers and its variability.
 415
 416 Table 5. Mean annual rock surface temperature (MARST) recorded at six different site on Mt. Ortles. Site
 417 locations are reported in Fig. 1. MARST is reported only for years with less than one month of missing data,
 418 and is calculated between the 1st of September and the 31st of August.
 419

LOCATION	CIMA_ALTO			CIMA_VERTICALE			ANTICIMA_SUD			BIVACCO_LOMBARDI			HINTERGRAT			PAYER			
	0.10	0.30	0.55	0.10	0.30	0.55	0.10	0.30	0.55	0.10	0.30	0.55	0.10	0.30	0.55	0.10	0.30	0.55	
Depth (m)																			
Year																			
2012	-2.1	-2.3	-2.6	-2.6	-2.5	-2.5	-1.8	-2.2	-2.7	-2.4	-2.3	-2.4							
2013	-2.0	-2.3	-2.5	-3.1	-3.1	-3.0	-3.1	-3.5	-3.9	-2.8	-2.7	-2.7	-2.2	-2.1	-2.2	1.4	1.2	0.9	
2014				-2.9	-2.8	-2.8	-2.5	-2.8	-3.3	-2.8	-2.7	-2.7				1.8	1.5	1.2	
2015				-2.1	-2.1	-2.1	-2.2	-2.6	-3.1	-1.5	-1.4	-1.6				2.7	2.4	2.1	
2016				-2.4	-2.3	-2.3	-2.2	-2.5	-3.0	-3.2	-3.1	-3.1				1.9	1.6	1.3	

420
 421
 422
 423
 424



425

APPENDICES

426

427 APPENDIX A: Variables in data files

428 Table A1. Column names for variables reported in data files.

Variable	Column name
Air temperature (fan-aspirated Vaisala HMP155A)	Air_T_HMP_Asp
Air temperature (natural-ventilation Vaisala HMP155A)	Air_T_HMP_Nat
Air temperature (fan-aspirated Gemini TGP-4020)	Air_T_TGP_Asp
Air temperature (natural-ventilation Gemini TGP-4020)	Air_T_TGP_Nat
Air temperature (natural-ventilation Onset Hobo H8 Pro Temp)	Air_T_H8_Nat
Englacial temperature at the AWS site	AWS_En (depth m)
Englacial temperature at the borehole drilling site (short string)	BH_En_SS (depth m)
Englacial temperature at the borehole drilling site (long string)	BH_En_LS (depth m)
Englacial temperature at the Hintergrat Glacier	HG_En (depth m)
Soil surface temperature at bivouac Lombardi - ORTL_05	GST_ORTL05
Soil surface temperature at bivouac Lombardi - ORTL_06	GST_ORTL06
Soil surface temperature at refuge Payer - ORTL_07	GST_ORTL07
Soil surface temperature at refuge Payer - ORTL_08	GST_ORTL08
Soil surface temperature at Hintergrat ridge - ORTL_10	GST_ORTL10
Soil surface temperature at Hintergrat ridge - ORTL_11	GST_ORTL11
Rock wall temperature at Mt. Ortles summit - CIMA_ALTO	Rw_ALTO (depth m)
Rock wall temperature Mt. Ortles summit - CIMA_VERTICALE	Rw_VERTICALE (depth m)
Rock wall temperature at Vorgipfel - ANTICIMA_SUD	Rw_ANTICIMA (depth m)
Rock wall temperature at bivouac Lombardi - BIV_LOMBARDI	Rw_LOMBARDI (depth m)
Rock wall temperature at Hintergrat - HINTERGRAT	Rw_HINTERGRAT (depth m)
Rock wall temperature at refuge Payer - PAYER	Rw_PAYER (depth m)

429



430

431 **APPENDIX B: Quality flags for data files**

432 Table B1. Quality code flags reported in data files, their meaning and explanations.

Quality code flag (“_FI” inflection in column names)	Meaning	Explanation
1	Good data	No issues detected during quality checks
0	No data	Data missing or removed (malfunctioning, physically implausible, sensor/device damaged, sensor underneath snow)
2	Maintenance	Data are affected by field maintenance of instrumentation
3	Ice/snow accretion	The air temperature data are affected by ice or snow accretion
4	Small height of the sensor	The air temperature sensor is less than 1 m above the snow surface
5 (offset)	Sensor offset	Offset applied to correct soil surface temperature data, based on the zero-curtain phase during snow melt (offset value in brackets)

433

434

435

436 **APPENDIX C: Data files structure**

437 Table C1. Structure of data files. For sensors at different depth below the surface, the depth in m is reported
 438 after the variable name, in brackets.

Date and hour (UTC)	Variable name (depth m)	Quality flag code
DD/MM/YYYY HH:MM	value	code

443

444

445 **APPENDIX D: Maintenance logs**

446 Table D1. Field operations and maintenance for the air temperature sensors mounted at the AWS on Mt. Ortelles.

Date	Field operations
01/10/2011	AWS setup and datalogger launch
18/06/2012	Datalogger download, check of sensor status and functioning
07/09/2012	Datalogger download, check of sensor status and functioning, 2 m increase in height of support tower, installation of two additional sensors (Vaisala HMP155A with natural ventilation, and Onset Hobo H8 Pro Temp)
01/07/2013	Datalogger download, check of sensor status and functioning. The fan-aspirated radiation shield was found damaged and not working



03/09/2013	Datalogger download, check of sensor status and functioning, 2 m increase in height of support tower. The fan-aspirated radiation shield was repaired and resumed working properly
03/07/2014	Datalogger download, check of sensor status and functioning
23/09/2014	2 m elongation of support tower. Sensors have been partially buried by snow between 2 and 23/09/2014
29/06/2015	Datalogger download, check of sensor status and functioning. Support tower lengthened by 2 m. Sensors have been partially buried by snow between 15 and 29/06/2015. Removal of all sensors except the Onset Hobo H8 Pro Temp
31/08/2015	Onset Hobo H8 Pro Temp download, check of sensor status and functioning
02/09/2016	Onset Hobo H8 Pro Temp download, check of sensor status and functioning. Sensor removed

447

448

449 Table D2. Field operations and maintenance for the englacial temperature sensors installed on Mt. Ortles.

Date	Field operations
17/11/2011	Installation and launch of the Sommer thermistor strings at the borehole drilling site and at the Hintergrat Glacier.
18/06/2012	Installation and launch of the Geoprecision thermistor string at the AWS site. Download and maintenance (battery replacement) of the Sommer thermistor strings at the borehole drilling site
28/08/2012	Download and maintenance (battery replacement) of the Sommer thermistor string at the Hintergrat Glacier. Sensor at 7.5 m initial depth stopped working on 18/08/2012
07/09/2012	Download of the Geoprecision thermistor string at the AWS site. Download and maintenance (battery replacement) of the Sommer thermistor strings at the borehole drilling site
01/07/2013	Download of the Geoprecision thermistor string at the AWS site. Download and maintenance (battery replacement, logger raised to the surface) of the Sommer thermistor strings at the borehole drilling site
23/08/2013	Download and maintenance (battery replacement) of the Sommer thermistor string at the Hintergrat Glacier. The sensor at 1.5 m initial depth was above the glacier surface
03/09/2013	Download of the Geoprecision thermistor string at the AWS site. Download and maintenance (battery replacement) of the Sommer thermistor strings at the borehole drilling site. Long string stopped working on 10/04/2013
03/07/2014	Download and maintenance (battery replacement, logger replacement) of the short Sommer thermistor string at borehole drilling site. Removal of the datalogger of the long Sommer thermistor string at borehole drilling site (no longer working).
28/08/2014	Download and maintenance (battery replacement) of the Sommer thermistor string at the Hintergrat Glacier. Sensor at 5.5 m initial depth stopped working on 17/08/2014
23/09/2014	Download and maintenance (battery replacement, logger raised to the surface) of the short Sommer thermistor string at the borehole drilling site
18/10/2014	Download of the Geoprecision thermistor string at the AWS site
29/06/2015	Download of the Geoprecision thermistor string at the AWS site
27/08/2015	Download and maintenance (battery replacement) of the Sommer thermistor string at the Hintergrat Glacier
31/08/2015	Download and removal of the short Sommer thermistor string at the borehole drilling site
23/08/2016	Download and removal of the Sommer thermistor string at the Hintergrat Glacier
02/09/2016	Download of the Geoprecision thermistor string at the AWS site

450



451

452 Table D3. Field operations and maintenance for the soil surface temperature sensors installed on Mt. Ortles.

Date	Field operations
02/09/2010	Installation and launch of the ORTL_05, ORTL_06, ORTL_07 and ORTL_08 Gemini TGP-4020
23/09/2010	Installation and launch of the ORTL_10 and ORTL_11 Gemini TGP-4020
28/08/2012	Download and maintenance (battery replacement, logger re-launch) at the ORTL_07, ORTL_08, ORTL_10 and ORTL_11
07/09/2012	Download and maintenance (battery replacement, logger re-launch) at the ORTL_05 and ORTL_06
23/08/2013	Download and maintenance (battery replacement, logger re-launch) at the ORTL_07, ORTL_08, ORTL_10 and ORTL_11
03/09/2013	Download and maintenance (battery replacement, logger re-launch) at the ORTL_05 and ORTL_06
28/08/2014	Download and maintenance (battery replacement, logger re-launch) at the ORTL_07, ORTL_08 and ORTL_10. ORTL_05, ORTL_06 and ORTL_11 not found, buried by snow
27/08/2015	Download and maintenance (battery replacement, logger re-launch) at the ORTL_07, ORTL_08 and ORTL_10
31/08/2015	Download and maintenance (battery replacement, logger re-launch) at the ORTL_05 and ORTL_06
23/08/2016	Download and removal of the ORTL_07, ORTL_08 and ORTL_10
02/09/2016	Download and removal of the ORTL_05 and ORTL_06

453

454

455 Table D4. Field operations and maintenance for the rock wall temperature sensors installed on Mt. Ortles.

Date	Field operations
30/08/2011	Installation and launch of the Geoprecision thermistor strings at CIMA_ALTO, CIMA_VERTICALE, ANTICIMA_SUD, BIV_LOMBARDI
14/10/2011	Installation and launch of the Geoprecision thermistor string at HINTERGRAT
28/11/2011	Installation and launch of the Geoprecision thermistor string at PAYER
28/08/2012	Download of thermistor strings at HINTERGRAT and PAYER. Repair of the Geoprecision thermistor string at HINTERGRAT
07/09/2012	Download of thermistor strings at CIMA_ALTO, CIMA_VERTICALE, ANTICIMA_SUD, BIV_LOMBARDI
23/08/2013	Download of thermistor strings at HINTERGRAT and PAYER
03/09/2013	Download of thermistor strings at CIMA_ALTO, CIMA_VERTICALE, ANTICIMA_SUD, BIV_LOMBARDI
28/08/2014	Download of thermistor string at PAYER
01/09/2014	Download of thermistor strings at HINTERGRAT, damaged, removed
27/08/2015	Download of thermistor string at PAYER
31/08/2015	Download of thermistor strings at CIMA_ALTO, CIMA_VERTICALE, ANTICIMA_SUD, BIV_LOMBARDI. CIMA_ALTO damaged, removed
23/08/2016	Download and removal of the thermistor string at PAYER
02/09/2016	Download and removal of the thermistor strings at CIMA_VERTICALE, ANTICIMA_SUD, BIV_LOMBARDI

456

457



458 **APPENDIX E: Characteristics of measurement sites**

459 Table E1. Topographic and geomorphological characteristics of sites instrumented for temperature

460 measurements.

Measured variable	Elevation (m a.s.l.)	East coordinate UTM WGS84 (m)	North coordinate UTM WGS84 (m)	Aspect	Slope (degrees)	Site description
Air Temperature (automatic weather station)	3830	618254	5151614	NW	11	Upper accumulation area of Alto dell'Ortles Glacier
Snow and firn temperature at the AWS site	3830	618260	5151619	NW	11	Upper accumulation area of Alto dell'Ortles Glacier
Englacial temperature at the borehole drilling site (short and long strings)	3859	618373	5151536	W	7	Upper accumulation area of Alto dell'Ortles Glacier
Englacial temperature at the Hintergrat Glacier	3476	619435	5151395	N	12	Hintergrat Glacier
Soil surface temperature at Lombardi bivouac - ORTL_05	3351	618202	5152846	SW	7	Northern ridge of Mt. Ortles, bedrock covered by a thin layer of debris (fine gravel, sand)
Soil surface temperature at Lombardi bivouac - ORTL_06	3371	618284	5152772	N	22	Northern ridge of Mt. Ortles, recently deglaciated bedrock covered by a discontinuous layer of loose debris (fine gravel, sand)
Soil surface temperature at Payer - refuge ORTL_07	2994	618361	5153936	N	22	Northern ridge of Mt. Ortles, bedrock covered by a thick layer of debris (pebbles, gravel, sand) with sparse vegetation
Soil surface temperature at Payer - refuge ORTL_08	2899	618287	5154105	W	36	Northern ridge of Mt. Ortles, bedrock covered by coarse debris with isolated areas of thinner debris (fine sand and silt).
Soil surface temperature at Hintergrat ridge ORTL_10	3460	619628	5151341	S	22	Eastern ridge of Mt. Ortles, bedrock covered by a layer of debris (fine gravel, sand).
Soil surface temperature at Hintergrat ridge ORTL_11	3466	619491	5151374	SE	11	Eastern ridge of Mt. Ortles, bedrock covered by a thin layer of coarse debris (gravel, sand), close to the edge of the Hintergrat Glacier
Rock wall temperature at Mt. Ortles summit - CIMA_ALTO	3900	618512	5151691	E	70	70 m south of Mt. Ortles summit (3905 m), in a sub-vertical rock face about 30 m below the crest edge
Rock wall temperature Mt. Ortles summit - CIMA_VERTICALE	3880	618512	5151691	E	90	70 m south of Mt. Ortles summit (3905 m), in a vertical rock face about 50 m below the ridge, 20 m below CIMA_ALTO
Rock wall temperature at Vorgipfel - ANTICIMA_SUD	3810	618327	5151269	S	90	Vertical rock face, about 10 m below the upper rock wall edge
Rock wall temperature at Lombardi bivouac - BIV_LOMBARDI	3351	618213	5152784	W	70	Northern ridge of Mt. Ortles, sub-vertical rock wall, about 30 m below the crest edge
Rock wall temperature at Hintergrat - HINTERGRAT	3370	619710	5151334	NE	90	Eastern ridge of Mt. Ortles, vertical rock wall, about 10 m below the crest edge
Rock wall temperature at Payer refuge - PAYER	3030	618372	5153812	SE	90	Northern ridge of Mt. Ortles, vertical rock wall, about 20 m below the crest edge



461

462 **APPENDIX F: Description of the measuring equipment for air temperature**

463



464

465 Figure F1. The automatic weather station (AWS) installed on Mt. Ortles, whose summit is visible in the

466 background. The stake behind the weather station indicates the site of the Geoprecision thermistor string. Photo

467 taken on 7 September 2012, after the lengthening of the support tower.

468

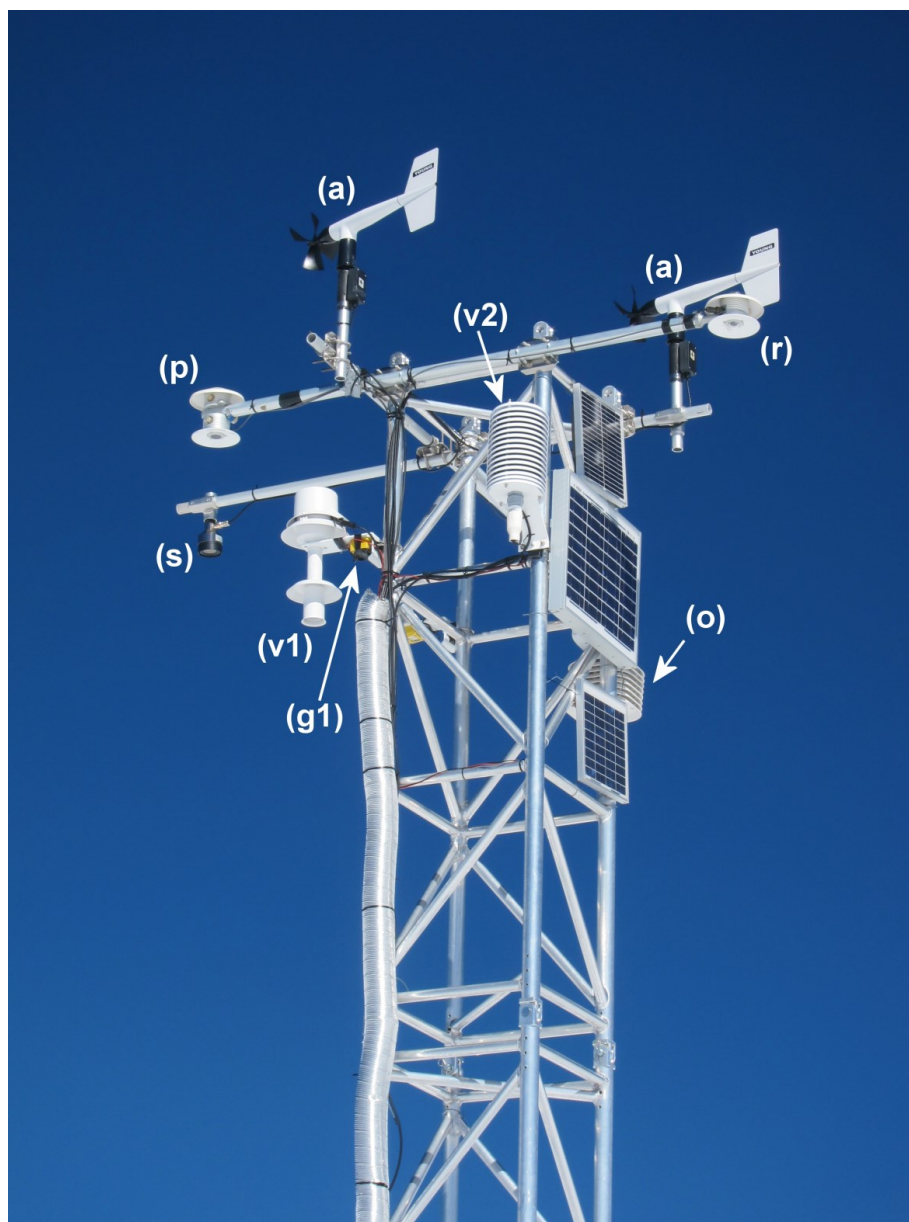


469

470 Figure F2. The wooden boards placed at the bottom of the support aluminum tower, at 2 m depth in the firm,

471

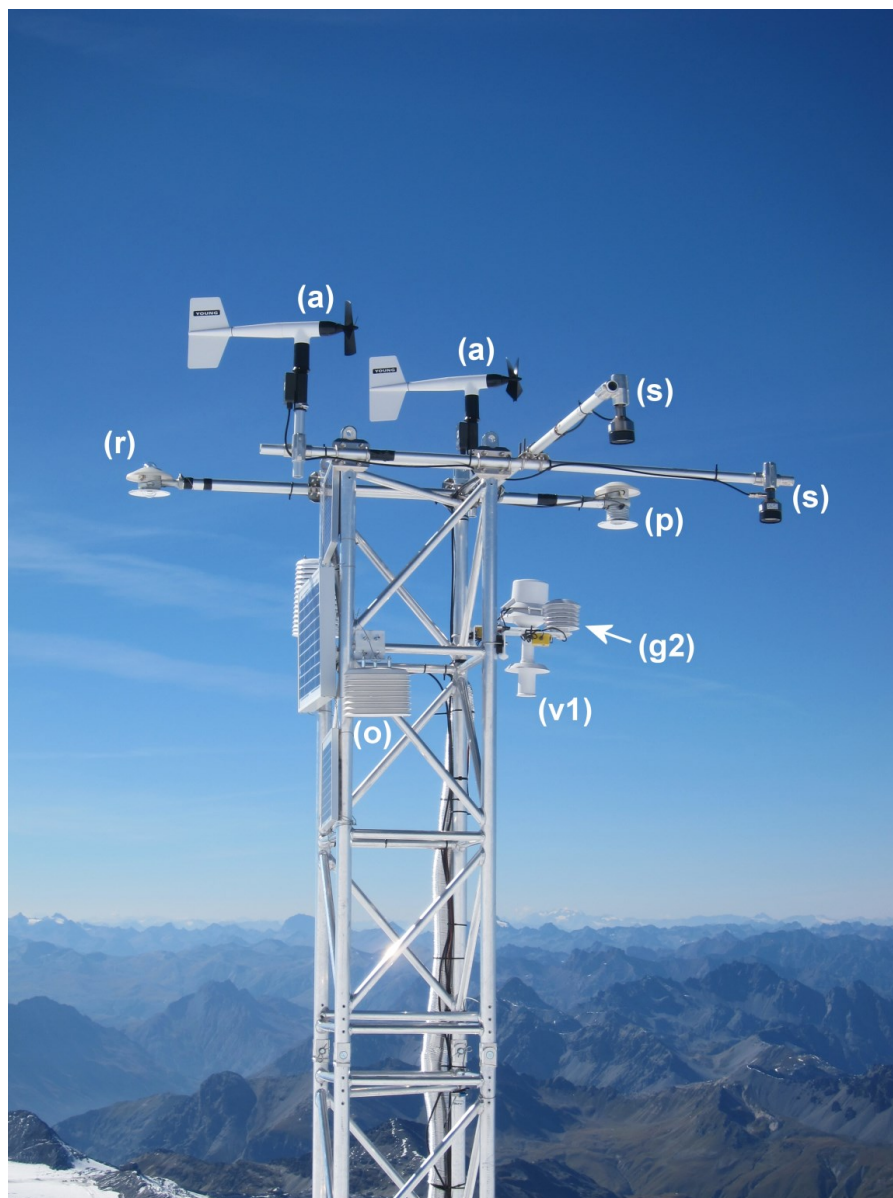
during the AWS installation. Photo taken on 30 September 2011.



472
473 Figure F3. Detail of the AWS seen from the west: a) R. M. Young 05103 anemometers, p) Delta Ohm LP
474 PIRG 01 pyrogeometers, r) Delta Ohm LP Pyra 05 radiometers, s) Campbell Scientific SR50A snow depth
475 sensors, v1) Vaisala HMP155A inside the R. M. Young 43502 fan-aspirated radiation shield, g1) Gemini TGP-
476 4020 datalogger inside the R. M. Young 43502 fan-aspirated radiation shield, v2) Vaisala HMP155A inside
477 the 15-plates Campbell Scientific MET 21 radiation shield with natural ventilation, o) Onset Hobo H8 Pro



478 Temp datalogger inside the 8-plates Davis 7714 radiation shield with natural ventilation. Photo taken on 7
479 September 2012.
480
481



482
483 Figure F4. Detail of the AWS seen from the east: a) R. M. Young 05103 anemometers, p) Delta Ohm LP PIRG
484 01 pyrogeometers, r) Delta Ohm LP Pyra 05 radiometers, s) Campbell Scientific SR50A snow depth sensors,



485 v1) Vaisala HMP155A inside the R. M. Young 43502 fan-aspirated radiation shield, g2) Gemini TGP-4020
486 datalogger inside the 6-plates R.M. Young 41303-5 radiation shield with natural ventilation, o) Onset Hobo
487 H8 Pro Temp datalogger inside the 8-plates Davis 7714 radiation shield with natural ventilation. Photo taken
488 on 7 September 2012.

489

490

491

492

493 **APPENDIX G: Description of the measuring equipment for englacial temperature**

494



495

496 Figure G1. The drilling site seen from the summit of Mt. Ortles. The Vorgipfel-Anticima Sud is visible in the
497 background. Photo taken on 1 October 2011 during the ice drilling operations, and before setting up the drilling
498 site thermistor strings for englacial temperature measurements.

499



500
501
502
503
504
505

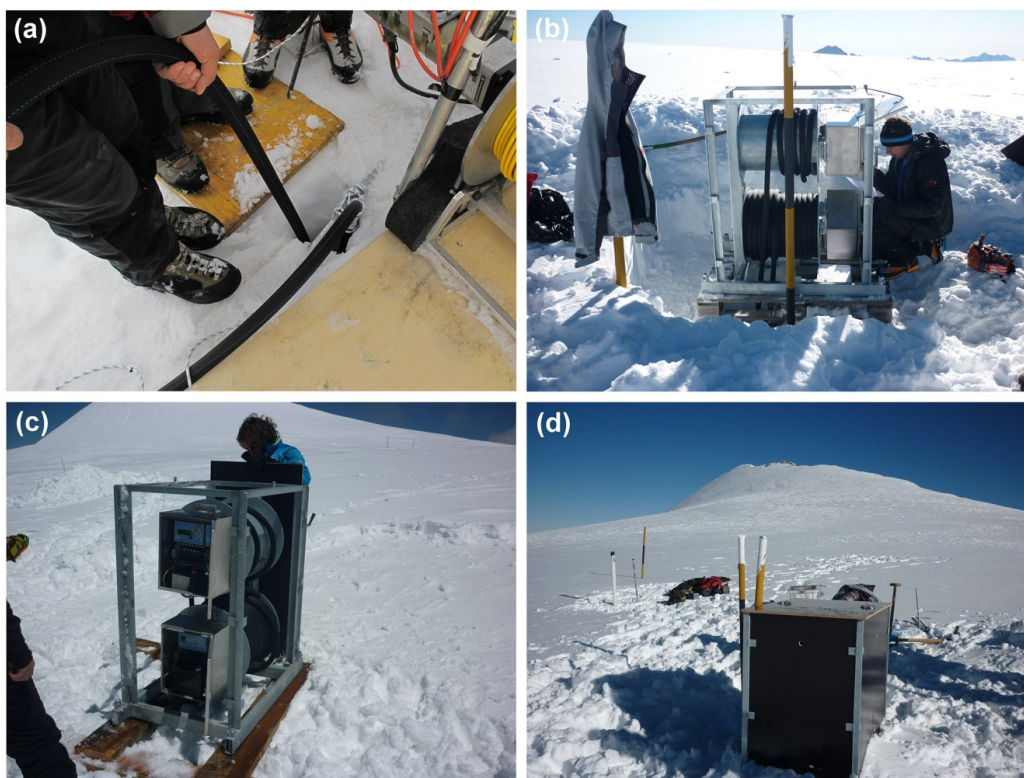


506
507 Figure G2. The Hintergrat Glacier seen from the south east (aerial photo taken on 28 August 2012). The black
508 asterisk indicates the location of the borehole equipped with the thermistor string.

509
510
511
512
513
514
515
516



517
518



519
520

521 Figure G3. a) Lowering of a thermistor string into the borehole n. 3 at the drilling site. b) The winding systems
522 of the two thermistor strings installed at the drilling site. c) The two metal boxes containing the thermistor
523 string data loggers and the batteries. d) Final arrangement of the box housing the winding systems and the data
524 loggers. The summit of Mt. Ortles is visible in the background. Photos taken on 17 November 2011.

525

526

527

528

529

530

531

532

533



534
535



536



537 Figure G4. a) Borehole drilling at the Hintergrat Glacier using a steam ice drill. b) The box containing the
538 winding system, the thermistor string data logger and the batteries. c) Final arrangement of the box housing
539 the winding systems and the data logger. Photos taken on 17 November 2011 and 27 August 2015.

540

541 **APPENDIX H: Description of the measuring equipment for soil surface temperature**

542

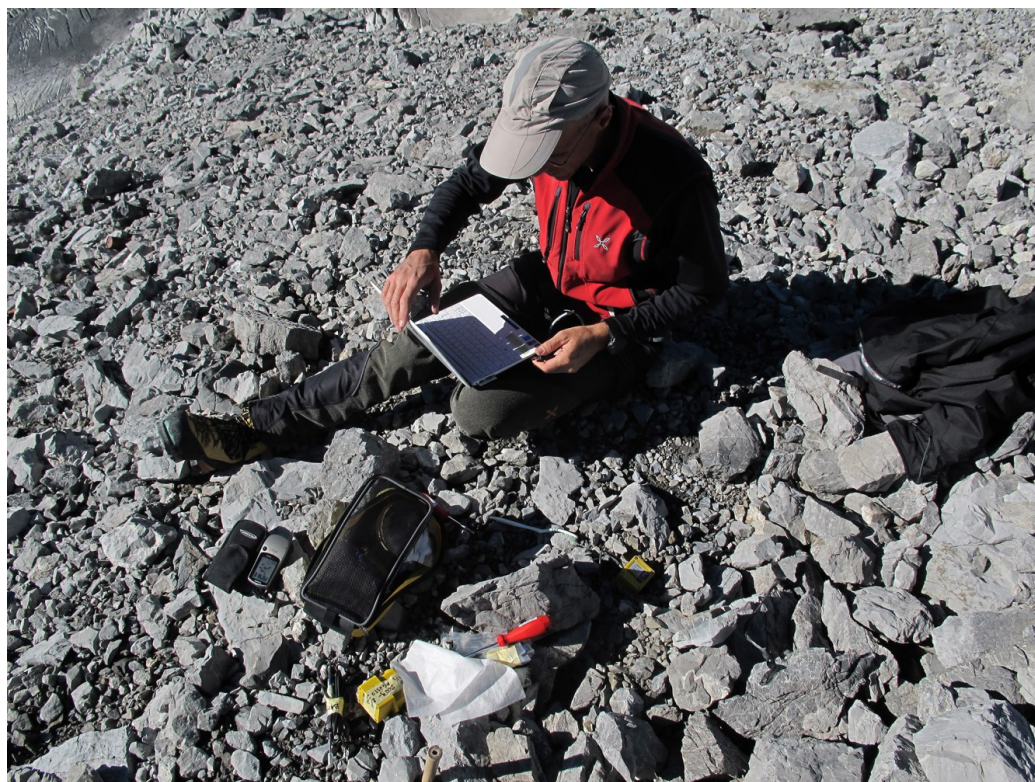


543
544 Figure H1. The soil surface temperature datalogger (Gemini TGP-4020) installed at the ORTL_05 site, close
545 to the Lombardi bivouac. The white ellipse indicates the PB-5001 external probe placed underneath the debris
546 surface. Photo taken on September 2010.

547

548

549



550

551 Figure H2. Data download and logger maintenance at the ORTL_10 soil surface temperature site on 28

552 August 2012.

553

554

555

556

557

558



559

560

561 Figure H3. Location of the six sites equipped with dataloggers for soil surface temperature measurement on

562 Mt. Ortles.

563

564



565

566 **APPENDIX I: Description of the measuring equipment for rock wall temperature**

567



568

569 Figure II. The rock wall temperature datalogger (Geoprecision thermistor string) installed close to the Payer
570 refuge. The datalogger is anchored to the rock wall and is connected to three temperature sensors placed at 0.1,
571 0.3 and 0.55 m depth inside a horizontal hole drilled in the rock wall. Photo taken on 28 November 2011.



572



573

574

575 Figure I2. Launching of the CIMA ALTO data logger. A wireless USB dongle secures the wireless

576 connection to the laptop used for launching the logger and for downloading the temperature data. Photo

577 taken on 30 August 2011.

578



579



580

581

582 Figure I3. Location of the six sites equipped with data loggers for rock wall temperature measurement on Mt.

583 Ortles (BIV_LOMBARDI and HINTERGRAT from © Google Earth Pro 7.3 (2022)).

584

585



586 **Acknowledgements**

587 This work is a contribution to the Ortles Project, a program supported by two NSF awards no. 1060115 & no. 1461422
588 to The Ohio State University and by the Ripartizione Protezione Antincendi e Civile of the Autonomous province of
589 Bolzano in collaboration with the Ripartizione Opere idrauliche e Ripartizione Foreste of the Autonomous province of
590 Bolzano and the Stelvio National Park. This is Ortles Project publication 11 (www.ortles.org). The research was funded
591 by the Italian MIUR Project (PRIN 2010-11), "Response of morphoclimatic system dynamics to global changes and
592 related geomorphological hazards" (local and national coordinators G. Dalla Fontana and C. Baroni). The authors are
593 grateful to all the students, technicians and scientists who contributed to the field activities in the period from 2009 to
594 2016, the Alpine guides of the Alpinschule of Solda, the helicopter companies Airway, Air Service Center, Star Work
595 Sky and the Hotel Franzenshöhe for logistical support. The authors acknowledge the support of Vinicio Carraro (TeSAF
596 Department of the University of Padova) for the setup of the automatic weather station, and of Umberto Morra di Cella
597 and Paolo Pogliotti (ARPA Val d'Aosta) for the setup of the rock wall temperature dataloggers. The soil surface
598 temperature measured on Mt. Vioz were kindly provided by the Servizio Geologico of the Autonomous province of
599 Trento (Matteo Zumiani).

600

601

602 **References**

603

604 Ballantyne, C. K.: Periglacial geomorphology, John Wiley & Sons Ltd., Hoboken, NJ, USA, 472 pp., ISBN:
605 978-1-405-10006-9, 2018.

606

607 Boeckli, L., Brenning, A., Gruber, S., and Noetzli, J.: Permafrost distribution in the European Alps: Calculation
608 and evaluation of an index map and summary statistics, *The Cryosphere*, 6, 807–820,
609 <https://doi.org/10.5194/tc-6-807-2012>, 2012.

610

611 Bohleber, P., Wagenbach, D., Schöner, W., and Böhm, R.: To what extent do water isotope records from low
612 accumulation Alpine ice cores reproduce instrumental temperature series?, *Tellus B*, 65, 1–17,
613 <https://doi.org/10.3402/tellusb.v65i0.20148>, 2013.

614



- 615 Braithwaite, R. J., Zhang, Y., and Raper, S. C. B.: Temperature sensitivity of the mass balance of mountain
616 glaciers and icecaps as a climatological characteristic, *Z. Gletsch.kd. Glazialgeol.*, 38, 35–61 pp., 2002.
617
- 618 Carturan, L.: Climate change effects on the cryosphere and hydrology of a high-altitude watershed, Ph.D.
619 thesis, TeSAF – University of Padova, 187 pp., 2010.
620
- 621 Carturan, L., Cazorzi, F., and Dalla Fontana, G.: Distributed mass-balance modelling on two neighbouring
622 glaciers in Ortles-Cevedale Italy, from 2004 to 2009, *J. Glaciol.*, 58, 467–486,
623 <https://doi.org/10.3189/2012JoG11J111>, 2012a.
624
- 625 Carturan, L., Dalla Fontana, G., and Borga, M.: Estimation of winter precipitation in a high-altitude catchment
626 of the Eastern Italian Alps: Validation by means of glacier mass balance observations, *Geogr. Fis. Din. Quat.*,
627 35, 37–48, <https://doi.org/10.4461/GFDQ.2012.35.4>, 2012b.
628
- 629 Carturan, L., Filippi, R., Seppi, R., Gabrielli, P., Notarnicola, C., Bertoldi, L., Paul, F., Rastner, P., Cazorzi,
630 F., Dinale, R., and Dalla Fontana, G.: Area and volume loss of the glaciers in the Ortles-Cevedale group
631 (Eastern Italian Alps): controls and imbalance of the remaining glaciers, *The Cryosphere*, 7, 1339–1359,
632 <https://doi.org/10.5194/tc-7-1339-2013>, 2013.
633
- 634 Carturan, L., De Blasi, F., Dinale, R., Dragà, G., Gabrielli, P., Mair, V., Seppi, R., Tonidandel, D., Zanoner,
635 T., Zandrini, T. L., and Dalla Fontana, G.: Data from air, englacial and permafrost temperature measurements
636 on Mt. Ortles (Eastern European Alps) (Version 1.0) [Data set]. Zenodo.
637 <https://doi.org/10.5281/zenodo.7879969>, 2023.
638
- 639 Charbonneau, R., Lardeau, J. P., and Obléd, C.: Problems of modelling a high mountainous drainage basin
640 with predominant snow yields, *Hydrol. Sci. B.*, 26, 345–361, <https://doi.org/10.1080/02626668109490899>,
641 1981.
642



643 Cicoira, A., Beutel, J., Faillettaz, J., Gärtner-Roer, I., and Vieli, A.: Resolving the influence of temperature
644 forcing through heat conduction on rock glacier dynamics: A numerical modelling approach, *The Cryosphere*,
645 13, 927–942, <https://doi.org/10.5194/tc-13-927-2019>, 2019.

646

647 Deline, P., Gruber, S., Delaloye, R., Fischer, L., Geertsema, M., Giardino, M., Hasler, A., Kirkbride, M.,
648 Krautblatter, M., Magnin, F., McColl, S., Ravel, L., and Schoeneich, P.: Ice Loss and Slope Stability in
649 High-Mountain Regions, *Snow and Ice-Related Hazards, Risks, and Disasters*, Academic Press, 521–561,
650 <https://doi.org/10.1016/B978-0-12-394849-6.00015-9>, 2015.

651

652 Gabrielli, P., Carturan, L., Gabrieli, J., Dinale, R., Krainer, K., Hausmann, H., Davis, M., Zagorodnov, V.,
653 Seppi, R., Barbante, C., Fontana, G. D., and Thompson, L. G.: Atmospheric warming threatens the untapped
654 glacial archive of Ortles mountain, South Tyrol, *J. Glaciol.*, 56, 843–853,
655 <https://doi.org/10.3189/002214310794457263>, 2010.

656

657 Gabrielli, P., Barbante, C., Carturan, L., Cozzi, G., Fontana, G. D., Dinale, R., Dragà, G., Gabrieli, J.,
658 Kehrwald, N., Mair, V., Thompson, L. G., and Tonidandel, D.: Discovery of cold ice in a new drilling site in
659 the eastern European Alps, *Geogr. Fis. Din. Quat.*, 35, 101–105, <https://doi.org/10.4461/GFDQ.2012.35.10>,
660 2012.

661

662 Gabrielli, P., Barbante, C., Bertagna, G., Bertó, M., Binder, D., Carton, A., Carturan, L., Cazorzi, F., Cozzi,
663 G., Dalla Fontana, G., Zanoner, T., and Zennaro, P.: Age of the Mt. Ortles ice cores, the Tyrolean Iceman and
664 glaciation of the highest summit of South Tyrol since the Northern Hemisphere Climatic Optimum, *The*
665 *Cryosphere*, 10, 2779–2797, <https://doi.org/10.5194/tc-10-2779-2016>, 2016.

666

667 Guglielmin, M., Aldighieri, B., and Testa, B.: PERMACLIM: A model for the distribution of mountain
668 permafrost, based on climatic observations, *Geomorphology*, 51, 245–257, [https://doi.org/10.1016/S0169-555X\(02\)00221-0](https://doi.org/10.1016/S0169-555X(02)00221-0), 2003.

670



671 Harris, C., Arenson, L. U., Christiansen, H. H., Etzelmüller, B., Frauenfelder, R., Gruber, S., Haeberli, W.,
672 Hauck, C., Hölzle, M., Humlum, O., Springman, S. M., and Vonder Mühll, D.: Permafrost and climate in
673 Europe: Monitoring and modelling thermal, geomorphological and geotechnical responses, *Earth Sci. Rev.*,
674 92, 117–171, <https://doi.org/10.1016/j.earscirev.2008.12.002>, 2009.

675

676 Huggel, C., Carey, M., Clague, J. J., and Kääh, A.: The high-mountain cryosphere: Environmental changes
677 and human risks, Cambridge University Press, 1–371 pp., <https://doi.org/10.1017/CBO9781107588653>, 2015.

678

679 Irvine-Fynn, T. and Hubbard, B.: Glacier Hydrology and Runoff, In *International Encyclopedia of Geography:*
680 *People, the Earth, Environment and Technology*, Elsevier,
681 <https://doi.org/https://doi.org/10.1002/9781118786352.wbieg0709>, 2017.

682

683 Knight, J. and Harrison, S.: The sensitivity and evolutionary trajectory of the mountain cryosphere:
684 Implications for mountain geomorphic systems and hazards, *Land Degrad. Dev.*,
685 <https://doi.org/10.1002/ldr.4630>, 2023.

686

687 Langsdorf, S., Löschke, S., Möller, V., Okem, A., Officer, S., Rama, B., Belling, D., Dieck, W., Götze, S.,
688 Kersher, T., Mangele, P., Maus, B., Mühle, A., Nabiyeva, K., Nicolai, M., Niebuhr, A., Petzold, J., Prentzler,
689 E., Savolainen, J., Scheuffele, H., Weisfeld, S., Weyer, N., Pörtner, H.-O., Roberts, D. C., Tignor, M.,
690 Poloczanska, E. S., Mintenbeck, K., Alegria, A., Craig, M., Langsdorf, S., Löschke, S., Möller, V., Okem, A.,
691 and Rama, B.: IPCC, 2022: Climate Change 2022: Impacts, Adaptation and Vulnerability. Working Group II
692 Contribution to the Sixth Assessment Report of the Intergovernmental Panel on Climate Change, Cambridge
693 University Press, Cambridge, UK and New York, NY, USA, 3056 pp.,
694 <https://doi.org/10.1017/9781009325844>, 2022.

695

696 Machguth, H., Purves, R. S., Oerlemans, J., Hoelzle, M., and Paul, F.: Exploring uncertainty in glacier mass
697 balance modelling with Monte Carlo simulation, *The Cryosphere*, 2, 191–204, [https://doi.org/10.5194/tc-2-](https://doi.org/10.5194/tc-2-191-2008)
698 191-2008, 2008.



699

700 Montrasio A, Berra F, Cariboni M, Ceriani M, Deichmann N, Ferliga C, Gregnanin A, Guerra S, Guglielmin
701 M, Jadoul F, Longhin M, Mair V, Mazzoccola D, Sciesa E, and Zappone A: Note illustrative della Carta
702 Geologica d'Italia - Foglio 024 Bormio, ISPRA, Roma, Italy, 16–26 pp., 2012.

703

704 Pepin, N., Bradley, R. S., Diaz, H. F., Baraer, M., Caceres, E. B., Forsythe, N., Fowler, H., Greenwood, G.,
705 Hashmi, M. Z., Liu, X. D., Williamson, S. N., and Yang, D. Q.: Elevation-dependent warming in mountain
706 regions of the world, *Nat. Clim. Change*, 5, 424–430, <https://doi.org/10.1038/nclimate2563>, 2015.

707

708 Pepin, N. C., Arnone, E., Gobiet, A., Haslinger, K., Kotlarski, S., Notarnicola, C., Palazzi, E., Seibert, P.,
709 Serafin, S., Schöner, W., Terzago, S., Thornton, J. M., Vuille, M., and Adler, C.: Climate Changes and Their
710 Elevational Patterns in the Mountains of the World, *Rev. Geophys.*, 60,
711 <https://doi.org/10.1029/2020RG000730>, 2022.

712

713 Rathore, N., Thakur, D., and Chawla, A.: Seasonal variations coupled with elevation gradient drives significant
714 changes in eco-physiological and biogeochemical traits of a high altitude evergreen broadleaf shrub,
715 *Rhododendron anthopogon*, *Plant Physiol. Bioch.*, 132, 708–719,
716 <https://doi.org/10.1016/J.PLAPHY.2018.08.009>, 2018.

717

718 World Meteorological Organization: Guide to Instruments and Methods of Observation, Volume I,
719 Measurement of Meteorological Variables (WMO No. 8), Geneva, Switzerland, 2021.